



Forecast and simulation of stratospheric ozone filaments: A validation of a high-resolution potential vorticity advection model by airborne ozone lidar measurements in winter 1998/1999

Birgit Heese, Sophie Godin, Alain Hauchecorne

► To cite this version:

Birgit Heese, Sophie Godin, Alain Hauchecorne. Forecast and simulation of stratospheric ozone filaments: A validation of a high-resolution potential vorticity advection model by airborne ozone lidar measurements in winter 1998/1999. *Journal of Geophysical Research: Atmospheres*, 2001, 106 (D17), pp.20011-20024. 10.1029/2000JD900818 . insu-03091690

HAL Id: insu-03091690

<https://insu.hal.science/insu-03091690>

Submitted on 31 Dec 2020

HAL is a multi-disciplinary open access archive for the deposit and dissemination of scientific research documents, whether they are published or not. The documents may come from teaching and research institutions in France or abroad, or from public or private research centers.

L'archive ouverte pluridisciplinaire **HAL**, est destinée au dépôt et à la diffusion de documents scientifiques de niveau recherche, publiés ou non, émanant des établissements d'enseignement et de recherche français ou étrangers, des laboratoires publics ou privés.

Forecast and simulation of stratospheric ozone filaments: A validation of a high-resolution potential vorticity advection model by airborne ozone lidar measurements in winter 1998/1999

Birgit Heese,¹ Sophie Godin and Alain Hauchecorne

Service d'Aeronomie du Centre National de la Recherche Scientifique, Paris, France

Abstract. In the framework of the Third European Stratospheric Experiment on Ozone project Meridional Transport of Ozone in the Lower Stratosphere (METRO) an airborne ozone lidar has been flown on the French Falcon (Mystere 20) during winter 1998/1999 to investigate polar and subtropical filaments at midlatitudes. The objective of the METRO project is to quantify the proportion of the transport of polar and subtropical air and their mixing into midlatitude air masses. The dynamical evolution of the northern winter hemisphere was simulated using a high-resolution advection model for potential vorticity (PV): Modele Isentropique de transport Mesoechelle de l'Ozone Stratospherique par Advection (MIMOSA). To validate the model for further studies, it was first utilized to forecast the appearance of filaments inside the range of the airplane so that each flight of the airborne campaign could be planned precisely. The vertical ozone distribution measured along the flight tracks was then compared to the respective PV distribution simulated by the advection model. Correlation coefficients between 0.5 and 0.7 found over the altitude range where the filaments were observed show a good agreement between PV and ozone filaments. An improvement of the correlation up to 0.8 by horizontal shifting of the ozone profiles against the PV evolution showed that small displacements of less than 1° of the modeled PV filaments can occur. These displacements can be explained by the uncertainties of the input wind velocity data and of the lidar data. Thus we can conclude that the PV advection model MIMOSA reproduces the position, size, and structure of polar filaments and subtropical intrusions well in the range of the expected accuracy. The model is a suitable tool for further studies of the quantification of the global, long-term transport and mixing of polar and subtropical air into mid-latitudes.

1. Introduction

The decrease of total ozone at Northern Hemisphere midlatitudes is now a well-recognized fact [World Meteorological Organization, 1998]. The highest reduction rate of 6% per decade has been observed during winter and spring mainly in the lower stratosphere. During summer and autumn, these rates are lying at 3% per decade. One of the most probable mechanisms for this decrease is the transport of air out of the polar vortex that has been depleted for ozone or been prepared for ozone destruction by heterogeneous chemical reactions.

This transport occurs mainly through the formation of filaments or laminae at the edge of the vortex. But also intrusions of ozone-poor air coming from the subtropical tropopause region contributes to the ozone budget in the midlatitudes lower stratosphere [e.g., Holton *et al.*, 1995].

Reid and Vaughan [1991] and Reid *et al.* [1993] revealed the important role of polar filaments in the erosion of the vortex during spring. Most of the filaments were observed at the altitude range between 13 and 19 km, the region where also the highest ozone decrease has been observed. The amount of transport of ozone-depleted air masses out of the polar vortex into midlatitudes is still not sufficiently quantified. Norton and Chipperfield [1995] modeled the transport of polar stratospheric cloud (PSC)-activated air out of the polar vortex for three consecutive winters and found large variations between 10% and 50% of the air inside the vortex. The meridional transport of subtrop-

¹Now at Meteorological Institute, University of Munich, Munich, Germany.

ical air to midlatitudes is driven to a great extent by Rossby wave breaking in the lower stratosphere associated with tropopause folding events [Hood *et al.*, 1999]. Such transport from the subtropical upper troposphere to the midlatitude lower stratosphere occurs on isentropic surfaces and represents a net transport of ozone-poor air. It appears to contribute significantly to the observed decrease in ozone at midlatitudes. Statistical trend analyses of lower stratospheric zonal winds and potential vorticity (PV) compared to ozone trends by Hood *et al.* [1999] showed that an increase in anticyclonic, poleward, Rossby wave breaking events over the last 20 years is favored by the observed trends in the winds. Regression relationships between column ozone and 330 K PV deviations gave an estimation of the contribution to the observed ozone decrease at midlatitudes to up to 40% in February and 25% in March. This poleward transport of subtropical air can also be regarded to take place in form of filaments. One example was reported during the European Arctic Stratospheric Ozone Experiment winter 1992 when a deep lamina of extremely ozone-poor air moved from the subtropics to the edge of the polar vortex [Orsolini *et al.*, 1995]. Vaughan and Timmis [1998] analysis showed that below 400 K a lot of this laminae had originated in the subtropical troposphere.

A detailed description of the structure and frequency of both polar and subtropical filaments is needed to quantify the contribution of these filamentation processes to the observed ozone decrease in the midlatitude lower stratosphere. This was the aim of the Third European Stratospheric Experiment on Ozone (THESEO) project Meridional Transport of Ozone in the Lower Stratosphere (METRO): to improve the knowledge about the mechanisms involved in the meridional transport of air in the lower stratosphere and to estimate its impact on the ozone budget at middle latitudes. Observations of polar filaments and subtropical intrusions were obtained using a network of ground-based stations equipped with ozone, temperature, and aerosol lidars, ozone sondes, and lidars and radars for wind profiling. In addition, an ozone lidar on board the French Falcon (Mystere 20) was used for a special METRO airborne campaign during winter 1998/1999 to obtain detailed cross sections of the filaments. One objective of the METRO project was to investigate the stratospheric transport processes with high-resolution dynamical models. This implied the intercomparison of the models and the validation of the models results by the measurements. Such validations are important, since the models are meant to be used for global studies such as the evaluation of ozone loss through polar filamentation events. So it is crucial to assess first the ability of the models to reproduce real polar filaments and subtropical intrusions. In this study we present the validation of one of the models used in the METRO project, the Modele Isentropique de transport Mesoechelle de l'Ozone Stratospherique par Advection

(MIMOSA) model, developed at Service d'Aeronomie du Centre National de la Recherche Scientifique (CNRS): A. Hauchecorne *et al.*, Quantification of the transport of chemical constituents from the polar vortex to middle latitudes in the lower stratosphere using the high-resolution advection model MIMOSA and effective diffusivity, submitted to *J. Geophys. Res.*, 2001 (hereinafter referred to as (Hauchecorne *et al.*, submitted manuscript, 2001)). The validation is done by the airborne lidar measurements of ozone profiles and is based on the hypothesis that PV and ozone are well correlated in midlatitude lower stratosphere [see, e.g., Butchart and Remsberg, 1986].

A similar study was made by Flentje *et al.* [2000]. Airborne ozone measurements performed during the Second European Stratospheric Arctic and Midlatitude Experiment (SESAME) in 1994/1995 where compared to contour advection simulations (CAS). But this study is based on the postanalysis of already existing data by CAS simulation. The new approach followed in the METRO project was to forecast the filaments and then check their existence and the position with the airborne lidar. The previously mentioned study focused on the vortex edge, while we focus on the observation of filaments at midlatitudes. Further away from the polar vortex, the filaments are often stretched out long and thin and would not be predicted by the European Centre for Medium-Range Weather Forecasts (ECMWF) analysis. Thus a high-resolution model was needed to resolve the structures of the filaments at midlatitudes. It should also be mentioned that the winter 1998/1999 was one with very low ozone destruction so that mostly dynamical processes played a role for the ozone content in the observed filaments. Therefore the obtained measurements are particularly useful for the validation of dynamical models.

In this paper, two representative cases of filaments observed by the airborne lidar are presented in detail: one polar filament and one subtropical intrusion. The structures and position of these filaments are compared to and correlated with the results of the high-resolution PV-advection model. The other flights performed during winter 1998/1999 were analyzed as well, and the results will be considered in the discussion.

2. Instrumentation and Lidar System

Ozone profiles were measured using an airborne lidar by flying through polar filaments and subtropical intrusions during winter and spring 1999. The already experienced lidar Airborne Lidar for Tropospheric Ozone (ALTO) [Ancellet and Ravetta, 1998] was mounted on the French Falcon, the Mystere 20, for the first time and was used for measurements in the lower stratosphere for the METRO campaign. The flight base was the small airport Creil near Paris where the Mystere 20 is deployed. The plane has a range of about 1000 nautical miles, corresponding to 1852 km. Thus using this plane

from central Europe permits flying toward all directions and following a filament for about 2 days, depending on the direction it moves. The operational cruise altitude of the plane was around 33,000 feet, about 11 km.

The ALTO lidar consists of a solid-state neodymium: yttrium/aluminum/garnet (Nd:YAG) laser, frequency shifted to generate output in the UV (266 nm), working at a repetition rate of 20 Hz. A Raman cell is used for further wavelength conversion. The laser beam is emitted coaxial to the axis of a 40 cm Cassegrain telescope. The received signal is collected by a quartz optical fiber that transmits it to the entrance slit of a spectrometer. The three emitted wavelengths are separated by a holographic grating, and the signals are then collected by two photomultiplier tubes (PMT) for each wavelength. One of the PMTs is coupled to a photon counting unit and the other to an analog-to-digital conversion unit for optimization of the dynamical range of the system. Further details of the ALTO lidar are described by *Ancellet and Ravetta [1998]*.

For the ozone measurements in the lower stratosphere the differential absorption lidar (DIAL) method was applied using the wavelengths 299 and 341 nm, the first and second Stokes lines obtained by Raman conversion in H₂ of the fourth harmonic of a pulsed Nd:YAG laser, that is 266 nm. These wavelengths were chosen to maximize the altitude range of the measurements. Another possible choice of the wavelength pair would have been 289 nm and 316 nm using a mixture of D₂ and a buffer gas (He) for Raman conversion. These wavelengths were used for tropospheric measurements with

ALTO before. Since the ozone content in the stratosphere is much higher, 289 nm would have been absorbed too fast and the altitude range of the filaments above the airplane would not be covered. Thus 299 nm was chosen as the absorbing wavelength. Regarding the reference wavelength, different options were considered, 316, 328 and 341 nm, respectively, which can be easily achieved by Raman conversion using H₂ or D₂, or a mixture of both. Simulations of the receivable signal using a climatological polar and subtropical ozone profile were made to find the best reference wavelength. The background signal from the sky was assumed to be 0.1 pulses μs^{-1} for 316 nm, 0.6 pulses μs^{-1} for 328 nm, and 1.25 pulses μs^{-1} for 341 nm, respectively, with reference to former experience using 316 nm and taking the solar spectrum in the stratosphere into account. Regarding the precision of the ozone measurements, the choice of the reference wavelength did not make a significant difference (Figure 1). In contrast, the variation of the achieved outgoing energy of the wavelengths contributed much more to the expected precision of the ozone values. As shown by the upper curve in Figure 1, an increase in energy from 3 to 8 mJ for 299 nm leads to a significant improvement of the precision. In order to achieve the highest energy output at all wavelengths, several options of Raman shifting conditions were investigated. According to *de Schoulenikoff et al. [1997, Figure 7]*, the photon conversion efficiency of the first and second Stokes lines (S1 and S2) for single Raman scattering of the fourth harmonics of a Nd:YAG laser, 266 nm, has a sharp maximum (more than 50% for S1,

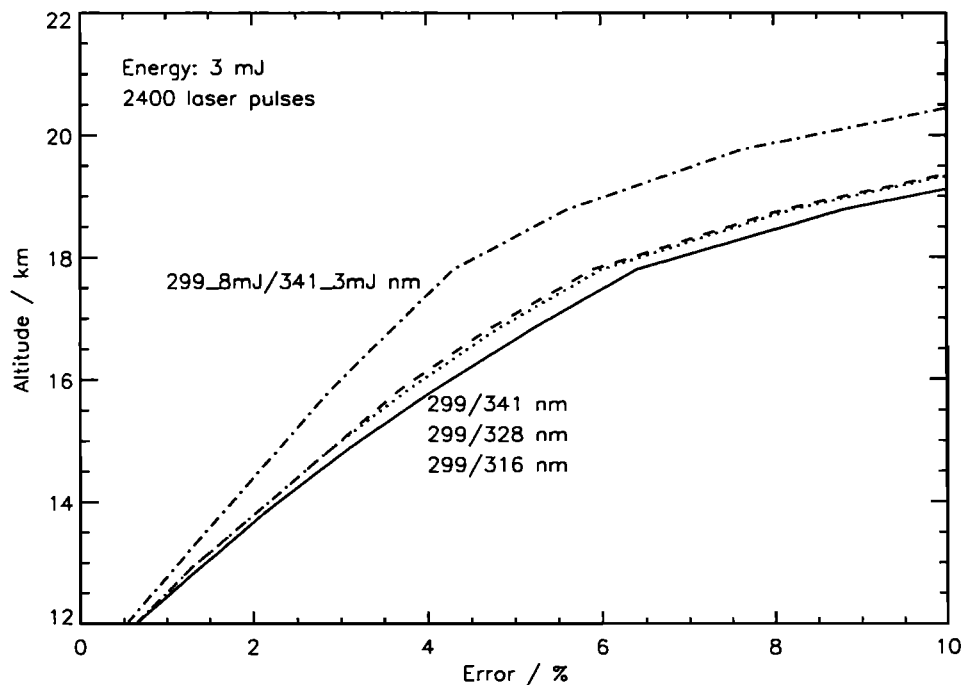


Figure 1. Simulation of lidar return signals for several wavelength pairs. The output energy was assumed to be 3 mJ for the three bottom curves, and 8 mJ at 299 nm and 3 mJ for 341 nm for the top curve.

Table 1. Energy of Wavelengths at the Output of the Cell after Raman Conversion^a

Total Pressure	266 nm	289 nm	299 nm	316 nm	328 nm	341 nm
<i>Using 4 bar H₂ + 10/13 bar D₂</i>						
14 bar	2.0	1.25	1.8	0.85	1.7	1.9
17 bar	1.85	1.45	1.65	1.35	1.7	1.5
<i>Using Pure H₂</i>						
2 bar	3.0	—	6.0	—	—	6.0
4 bar	1.9	—	3.4	—	—	5.5
6 bar	1.5	—	2.5	—	—	5.0
<i>Using 6 bar H₂ + He-buffer gas</i>						
15 bar	1.0	—	1.3	—	—	5.0
19 bar	1.1	—	2.5	—	—	4.9
22 bar	1.1	—	1.8	—	—	3.7

^aThe pump energy is 20 mJ. Units are mJ.

40% for S2) near 2 bar in pure hydrogen. For a mixture of H₂ and a buffer gas (He), *de Schoulepenkoff et al.* [1997, Figure 21] found the maximum efficiency of 35% for S1 conversion by adding 10 bar of He to 1.5 bar of H₂. The maximum for the second Stokes line was 36% by adding 5 bar He. *Papayannis et al.* [1998] found a 50% S1 conversion efficiency of the third harmonic of a Nd:YAG laser, 355 nm, at 7 bar H₂, and 33% for S2. A mixture of H₂ and D₂ allows using S1 (H₂), 299 nm and S2 (D₂), 316 nm, that would provide a lower sky background than 341 nm. In order to find the most suitable wavelength combination, some experiments consisting in varying the pressure of pure H₂, adding a buffer gas (He) to the Raman cell or use a mixing of H₂ and D₂ were carried out. The results are summarized in Table 1. The laser provided a pump energy of 20 mJ. The pressure of H₂ has been varied from 6 to 2 bar, showing a maximum energy at 2 bar. Using 6 bar H₂ and adding from 9 to 16 bar He did not lead to better results in output energy at the desired wavelengths. Using a mixture of 4 bar H₂ and 10 or 13 bar D₂ lead at least to an equilibrium in energy levels at all output wavelengths, but only of about 1.5 mJ. The maximum output energy for each wavelength reached about 6 mJ for 299 and 341 nm at 2 bar of H₂ which corresponds to about 30% photon conversion efficiency at both S1 and S2. Thus the latter wavelengths pair was used for the flights during the METRO campaign.

3. PV Advection Model

The PV advection model MIMOSA has been developed at Service d'Aéronomie du CNRS by Hauchecorne et al. (submitted manuscript, 2001). The model advects PV on several isentropic levels by the horizontal wind components on a *x-y* grid centered at the North Pole

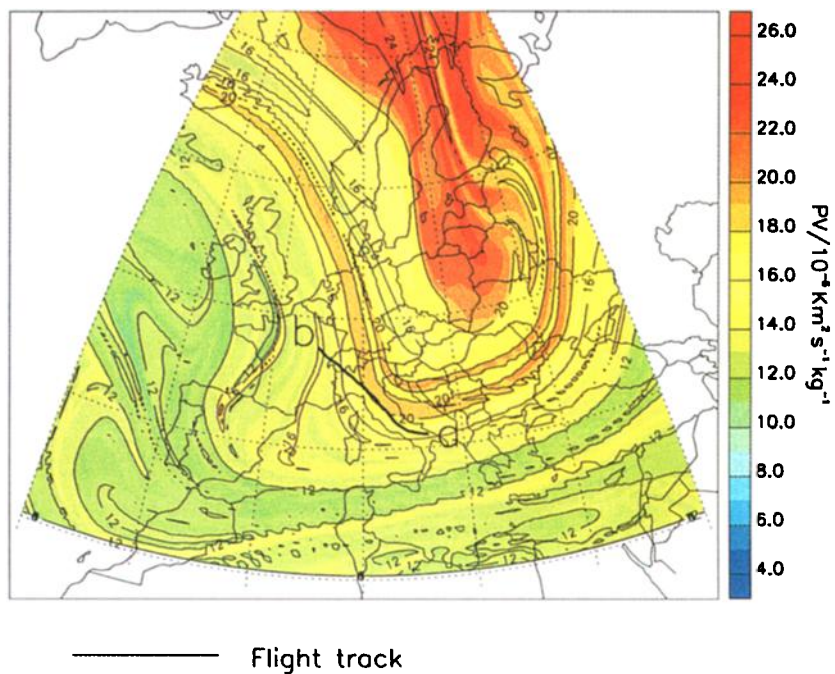
with a resolution of either 3 or 6 points per degree. The data field is then regridded every 6 hours onto the *x-y* grid points, to avoid empty areas due to diverging windtrajectories. The version of the model used in this study has been improved by reducing the numerical diffusion by the conservation of the second-order moment during interpolation onto the original grid after the advection. This new version of MIMOSA shows more detailed structures in the PV distribution.

A relaxation onto the ECMWF field is performed with a time constant of 10 days to consider the diabatic evolution of the PV field. The output field is given on latitude-longitude grid with a resolution of, again, either 3 or 6 points per degree.

3.1. Forecasting the Flights

As mentioned before, MIMOSA was used to predict the filaments and plan the individual flights during the airborne campaign. For this purpose the model was run using ECMWF wind and PV data at 1200 UTC provided by the Norwegian Institute for Air Research (NILU) Atmospheric Database for Interactive Retrieval (NADIR) with a resolution of 2.5° in both latitude and longitude. It delivered an analysis and 5 days forecasts of the PV distribution in the Northern Hemisphere north of 30°N. The model ran automatically every morning at 0500 UTC throughout the whole winter period providing the forecasts about 2 hours later. The flight alert procedure was as follows: If an interesting filament was forecasted to occur within the next 48 hours in the range of the airplane, a flight was planned for the respective day. If this filament was confirmed by the forecasts the day after, the flight was performed, unless weather conditions or flight restrictions did not allow the flight. In this manner the filaments could be

PV advection model MIMOSA on 18.02.1999 at level 435K



— Flight track

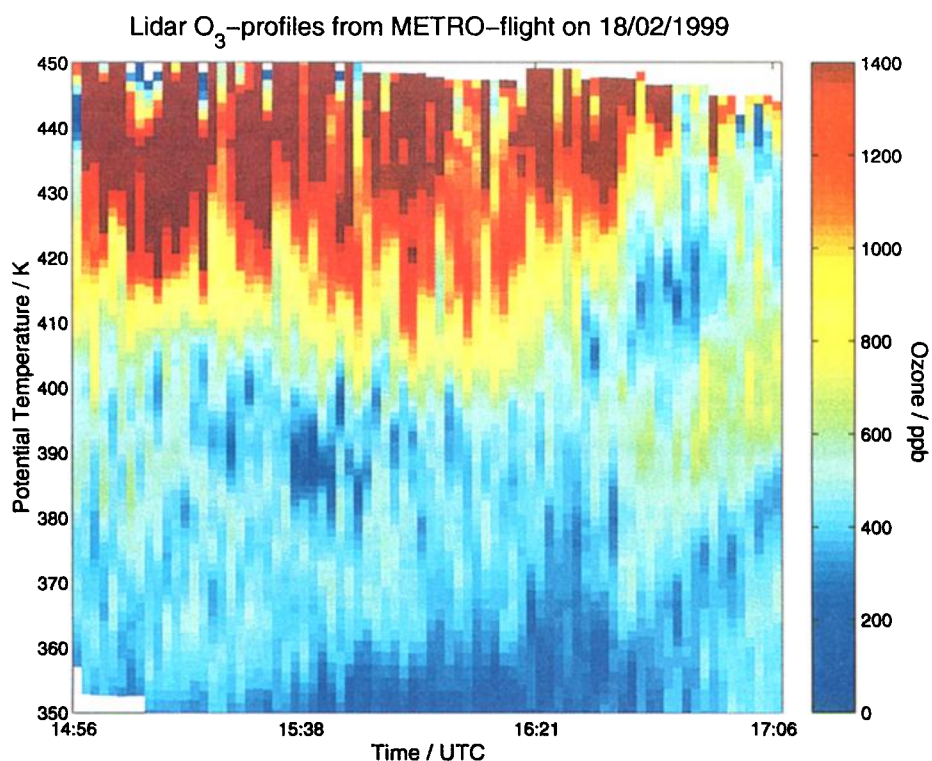


Plate 1. (top) Modeled PV distribution at 435 K on February 18, 1999 at 1600 UTC. The flight was performed from Brindisi, Italy (point a) to Paris (point b). (bottom) Measured ozone profiles during the flight on February 18, 1999.

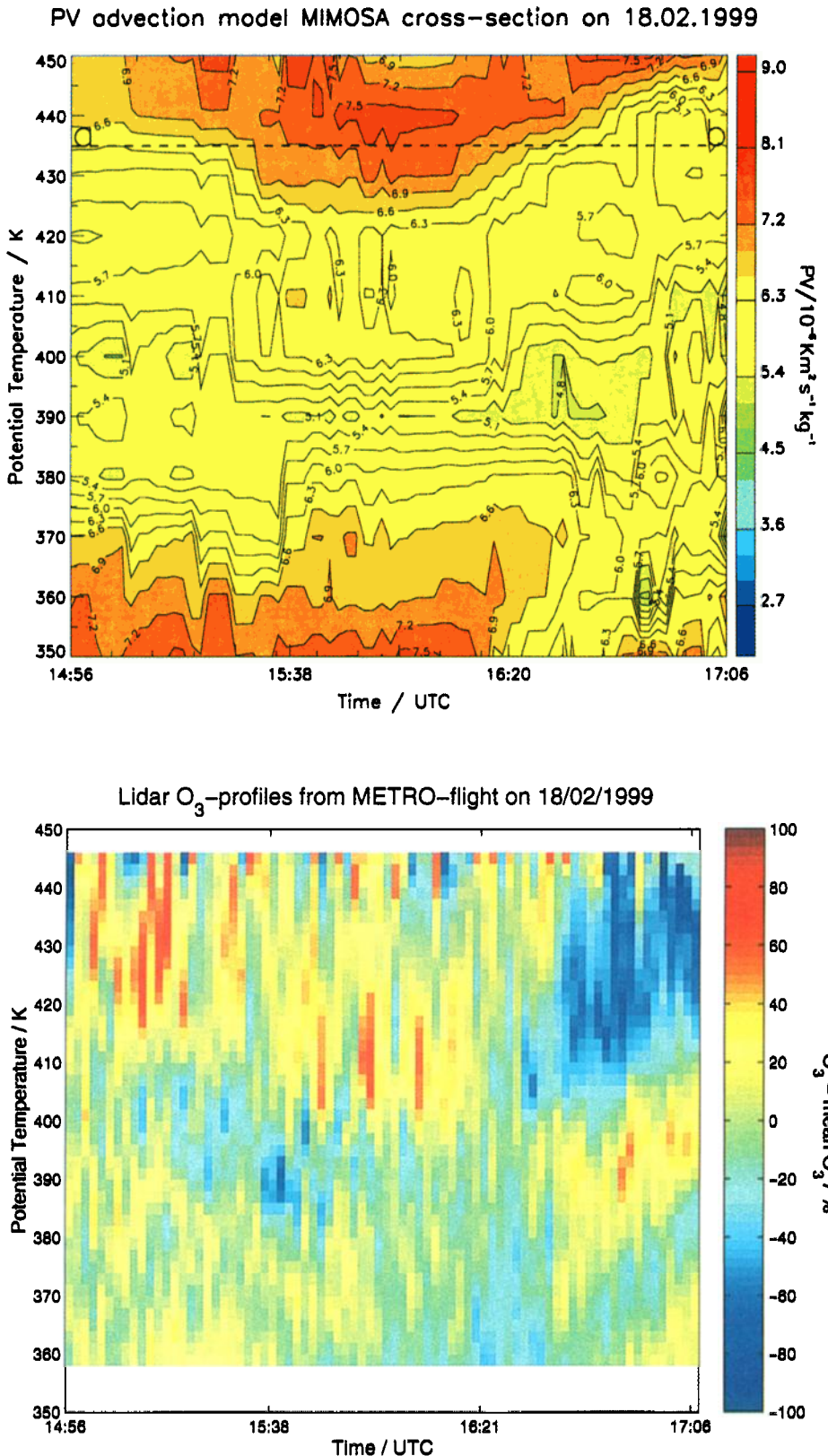


Plate 2. (top) Modified PV cross section during flight on February 18, 1999. The model MIMOSA was run on the levels 350 K to 450 K with a 10 K step. The dashed line indicates the level 435 K shown on the horizontal map in Plate 1. (bottom) Ozone anomalies calculated with respect to the mean ozone profile for this flight.

detected systematically, and the ones suitable for air-borne lidar measurements could be selected.

3.2. Data Interpretation

To compare the model results with the ozone data obtained during the flights, high-resolution ECMWF data (T106, corresponding to 1.125° on a regular latitude-longitude grid) were used. MIMOSA was run for a minimum of 10 days with a resolution of 6 points per degree for the advection grid and the output field was given for 3 points per degree. For the results presented in this paper T106 data were used every 6 hours at all synoptical observation times, 0000, 0600, 1200, and 1800 UTC.

For the comparison of the advected PV with the measured ozone profiles, a PV field of the European sector was extracted every hour on 11 isentropic levels, from 350 K to 450 K with a step of 10 K. Then the PV values obtained at every full hour before, during, and after the flight were interpolated onto the coordinates of the flight track to the time of each individual measurement of an ozone profile. Thus a cross section in time and isentropic level of the PV distribution during the METRO flights could be compared to the measured ozone profiles (see Plates 2 and 4, top panel).

4. Lidar Measurements During Winter 1998/1999

4.1. Stratospheric Situation

The northern hemispheric stratosphere during winter 1998/1999 was one of the dynamically most disturbed winters during the last decade [Naujokat, 1999]. This led generally to high temperatures in the polar region and a weak polar vortex. Although temperatures were cold and a strong polar vortex was observed in November, a major stratospheric warming occurred already in mid December and the polar region was covered by warm air throughout the stratosphere. During January, temperatures decreased slowly in the lower and middle stratosphere, but the circulation pattern remained disturbed. The next major warming developed during February, and in the beginning of March an anticyclonic flow was established at all levels of the stratosphere. A weak cyclonic circulation was reestablished at the end of March, and the transition to the summertime circulation was not completed before the beginning of May. The dynamically disturbed stratospheric circulation led to a lot of filamentation processes at the polar vortex edge and filaments of polar air masses could be observed frequently at midlatitudes during this winter. Thus several flights through polar filaments were performed toward south Italy (Brindisi) and in one case from Brindisi to Crete and Corsica and back to Paris. Some round trips over France and a flight to Ireland, from Ireland to Corsica and back to Paris, were performed through subtropical intrusions into midlatitude air.

4.2. Technical Problems

Since the lidar was mounted on the Mystere 20 for the first time, some minor problems occurred during the first flights. The plane had got a new window for the lidar looking upward into the stratosphere. When the temperature dropped below about -50°C outside the plane, the window was icing from the inside and the received signal got too weak. Going down in altitude with the plane toward warmer regions did help, but the deicing of the window was not fast enough to get sufficiently good data during the respective flight. Later the window was heated with warm air from the inside and no more icing problems occurred. Another problem were cirrus clouds above the planes flight altitude. For future flights a cirrus forecast should be taken into account during the planning of the flights. Due to flight and landing restrictions, in some cases we could not fly in the evening but had to fly during mid day. For these flights the background from the sky was getting a major problem, especially later in spring.

However, several flights with good data quality could be performed. In this paper we will investigate one example for each air mass type in detail. A typical polar filament was observed during the flight from Brindisi back to Creil on February 18, 1999. A subtropical intrusion could be measured during a round trip over France on March 29, 1999. The results of the other flights performed during this winter will be discussed together with these two examples in section 6.

4.3. Data Retrieval

The received lidar signals were analyzed using the DIAL method to calculate the ozone profiles. This method uses the difference in ozone absorption of the two emitted wavelengths, one absorbed highly by ozone (299 nm) and the other one very poorly, also called the reference wavelength (341 nm). This reference signal can be calculated when the atmospheric density profile is known, since only Rayleigh scattering contributes to the signal, and ozone absorption can be neglected. The ozone values measured in the case of a polar filament were calculated using the reference wavelength 341 nm. In the case of a subtropical intrusion, ozone values were sometimes so low that a sufficient difference in absorption between the two wavelengths could not be achieved, due to relatively low signal-to-noise ratio during daytime measurements. In these cases, instead of using the signal received at 341 nm, a reference signal was constructed using the density profile calculated from ECMWF analysis (T213) pressure and temperature data. An individual reference signal was used for each lidar profile taken along the respective flight track. Retrieving the lidar data this way leads to generally somewhat higher total ozone values, and some small-scale structures may be blurred out. In most cases the accuracy of the lidar data lies between 5% and 10%, depending on the sky background level. Data with

standard deviations exceeding 15% were not taken into account for the following correlations.

4.4. Comparison of Ozone and PV

To improve the visual comparison of the measured ozone profiles with the modeled PV filaments, anomalies were calculated using one mean ozone profile for each flight. The anomalies through a filament were compared to the corresponding modified PV cross section along the flight track. Modified PV is the PV normalized to a reference isentropic level:

$$\text{modified PV} = \text{PV} \left(\frac{\theta}{\theta_0} \right)^{\frac{1}{2}}, (\theta_0 = 350 \text{ K in this study})$$

and was applied to remove the dependence of PV on the increasing potential temperature with altitude [Lait, 1996].

4.4.1. Polar filament. During the flight on February 18, 1999, a polar filament originating from a tongue of the polar vortex over Scandinavia and eastern Europe, stretching from the Balkan over Italy and eastern France toward the North Sea, was crossed as shown on the horizontal PV distribution at the 435 K level (Plate 1, top). The ozone profiles measured during this flight are presented in Plate 1, bottom.

The filament can clearly be identified by the high ozone mixing ratios between 900 ppb and more than 1400 ppb at isentropic levels above 410 K. Toward the end of the flight the ozone mixing ratios at these levels drop down to values below 800 ppb, indicating that the filament has been left. Comparing the distribution of the ozone anomalies (Plate 2, bottom) with the modified PV distribution (top panel) reveals some more details of the filaments structure. The overall picture of the relative maxima in ozone at the higher isentropic levels, where the filament was observed, is reproduced well by the model. For example, the relative ozone maximum around 410 K between 1538 and 1620 UTC corresponds well with the PV maximum at this level. However, some small discrepancies occur: The maximum in ozone around 430 K in the beginning of the flight is not so pronounced in PV, while the PV maximum at higher levels also appears between 1538 and 1620 UTC, where the ozone anomalies show slightly lower values. The ozone minimum toward the end of the flight, representing midlatitude air mass outside the filament, is reproduced in PV as well. But the gradient in ozone appears to be steeper with altitude than the gradient in PV. Thus leaving the filament can be seen very well in PV and in ozone, but, from the point of view of one isentropic level, the model seems to be somewhat earlier.

4.4.2. Subtropical intrusion. On March 29, 1999, a circular flight over France was performed, when an intrusion of subtropical air was forecasted by the advection model. On the 380 K map (Plate 3) a ridge of an air mass with low PV is stretching northeastward over the Atlantic Ocean up to the British Isles and further

southeastward over France toward the Mediterranean Sea. The plane crossed this intrusion during the first half hour of the flight. At the levels from 360 K to 380 K a minimum in ozone was measured between 1620 and 1640 UTC. Above these levels, very low ozone values were observed between 390 K and 420 K. Indeed, they lay below the detection limit of the lidar that lies between 50 and 200 ppb depending on altitude and sky-light background. For the subtropical cases the error in ozone was increasing very fast and exceeding 10% as soon as the ozone values dropped below 200 ppb. So we set the detection limit for the subtropical flights to 200 ppb. During the remaining flight time a minimum of ozone could still be seen around these levels, but the values were slightly higher and lay around 300 ppb. The latter part of the flight shows a more or less symmetric pattern, since the plane turned about 90° and flew back through the same air mass.

Regarding the ozone anomalies (Plate 4) negative anomalies appear at levels around 400 K in the beginning of the flight and from 360 K to 370 K at 1630 UTC, as well as at 390 K at about 1640 UTC. The first minimum is reproduced by the model, but about 10 min earlier as observed in ozone. The same appears to be valid for the lower part around 360 K of the second, even deeper, minimum, although the minimum in PV is not so pronounced as the one in ozone. The upper part of this minimum is well located around 1630 UTC as is the minimum in PV. The third ozone minimum around 390 K can as well be associated with the low PV values around 1630 UTC stretching from level 370 K to 390 K. Also this minimum appears about 10 min earlier in PV than in ozone. The subtropical intrusion represented as an ozone minimum in the measurements is tilted forward in height between 360 K and 390 K, while the PV model shows a more vertical structure of the intrusion. The main flight track where the measurements were taken was in direction northeast, implying that the upper part of the subtropical intrusion was transported too slow by the model and placed about 100 km too far southwest of the observed ozone minimum.

5. Correlations Between Ozone and PV

The final goal of the METRO project is to quantify the transport and mixing of polar and subtropical air into midlatitude air and thus quantify the part of the observed decrease of ozone at midlatitudes that is caused by dynamical processes and the part due to real ozone destruction by chemically preprocessed air from polar regions. A correlation between the modeled PV and the measured ozone will give an indication how well the PV evolution as a tracer in the model MIMOSA represents the mixing of air masses taking place in the real atmosphere. The time evolution of the two values are correlated on the specific potential temperature levels where relevant structures of the filaments were

observed: i.e., around 435 K for polar filaments and around 380 K for subtropical intrusions.

5.1. Polar Filaments

For the polar flight on February 18, 1999, the correlations coefficients for the levels where the filament was observed are lying around 0.4 (430 K) to 0.6 (440 K). Reviewing the ozone data at the particular levels shows that they are quite noisy during the beginning of the flight (due to the higher skylight background). Removing these noisy data and starting the correlation later (at 1538 UTC) leads to a rise of the coefficients to around 0.7 at the levels from 420 K to 440 K. The comparison between the PV distribution and the ozone anomalies showed that the gradient by leaving the polar filament is found earlier in PV than measured in ozone. Shifting the ozone measurements by 500 s (100 km) back leads to an improvement of the correlation to 0.80 at 430 K. That confirms what was seen by comparing the ozone anomalies with the modified PV distribution: that the ozone gradient observed by leaving the filament is reproduced by the PV advection model but a little bit displaced.

The comparison of the ozone evolution along the flight track with the PV evolution for another polar filament observed on March 18, 1999, (Figure 2) implies a time shift of 300 s between both data sets that corresponds to a displacement of about 60 km. Also this flight was performed from Brindisi through a polar filament observed at latitudes relatively far south.

5.2. Subtropical Intrusions

In the case of a subtropical intrusion the lower levels around 380 K are the most interesting ones. On February 29, 1999 the ozone-poor air of the intrusion shows a sharp minimum at 360 K to 380 K. The correlation between ozone and PV at these levels gives a coefficient of 0.7 at 370 K and 0.5 at 380 K. At 370 K the ozone minimum is somewhat more narrow than the one in PV but located exactly where the minimum in PV occurs. This is reflected in the good correlation. At 380 K the minimum in ozone occurs about 500 s later than the minimum in PV and is somewhat wider (Figure 3). That means the gradient in ozone is not as sharp as in PV. At 390 K the ozone values are below the detection limit, and no correlation coefficient could be calculated. At 400 K the correlation of 0.6 is again quite well. Shifting the ozone values 500 s back and recorrelating the two fields leads to an improvement of the correlation to 0.6 at 380 K and to 0.8 at 400 K. At 370 K the correlation is getting worse (0.3), since the minimum in ozone will then be misplaced. The improvement of the correlation after shifting the ozone field backward in time at the upper levels of the filament reflects the tilt in the ozone minimum that has been suggested by the visual comparison of the ozone anomalies with the PV distribution. The main flight track where the measurements were taken was in direction northeast implying that the upper part of the subtropical intrusion was transported too slow by the model and placed about 100 km (i.e., 500 s) too far southwest.

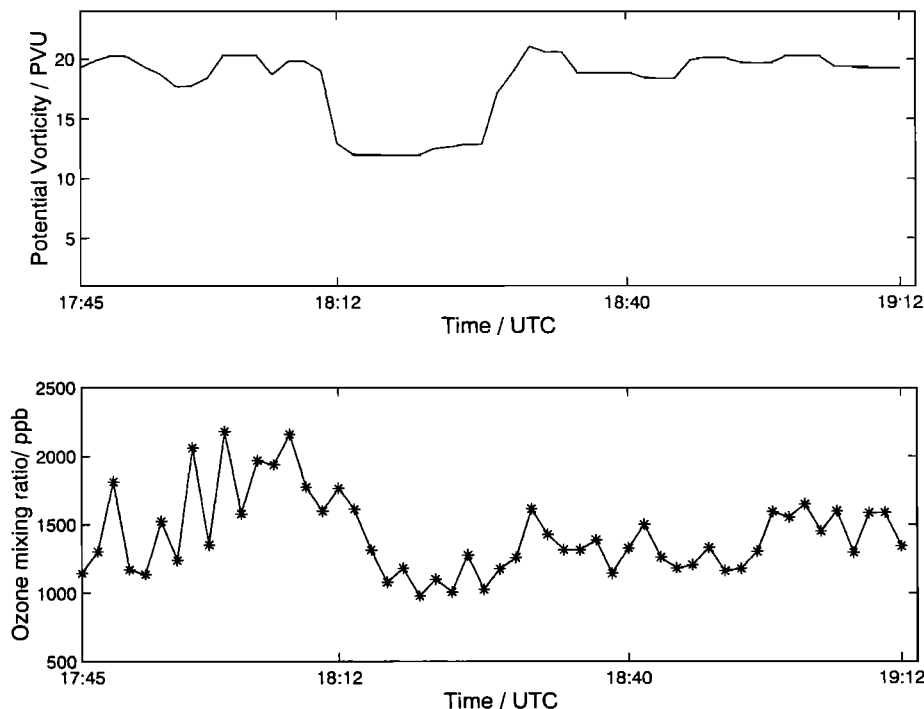


Figure 2. (top) Potential vorticity and (bottom) Ozone along the flight track on March 18, 1999 at 430 K. The stars indicate the ozone measurement taken every 100 s.

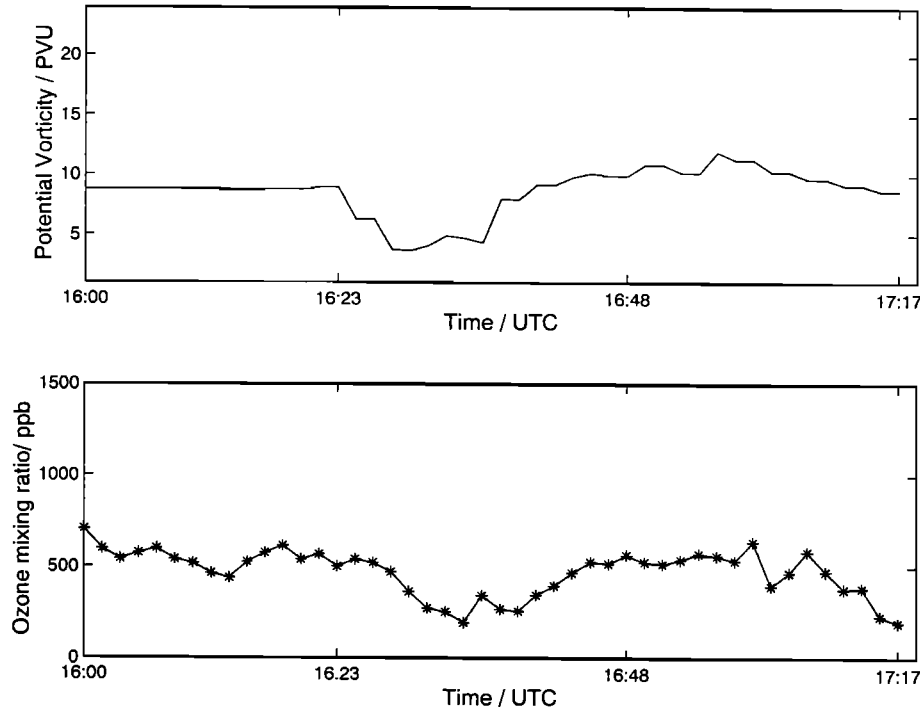


Figure 3. (top) Potential vorticity and (bottom) Ozone along the flight track on March 29, 1999 at 380 K.

For another subtropical intrusion observed over Ireland on April 6 and 7, 1999 the correlation of the measured ozone values with the modeled PV distribution on April 6 could be increased from 0.6 and 0.45 to 0.75 at the levels 380 K and 390 K, respectively, by shifting the PV field 25 min of the flight time against the ozone field. On April 7 an improvement of the correlation up to 0.7 at 370 K and 380 K could be achieved. The shift of 25 min into direction southeast corresponds to a misplacement of the subtropical intrusion of about 300 km too far west by the model. This is much more than found in the other cases, where the displacements of the filaments in PV were in the range of 60 to 100 km.

6. Discussion and Conclusions

Airborne lidar measurements of ozone filaments were undertaken systematically for the first time during winter 1998/1999 using the PV advection model MIMOSA to forecast the occurrence of polar and subtropical air masses in the midlatitude lower stratosphere. In all cases the predicted filaments were found in the measured ozone profiles. To quantify the ability of the model to reproduce the structure and geographical position of the real filaments, the ozone profiles have been compared to and correlated with the modeled PV filaments from MIMOSA. Already a visual inspection of the ozone and PV profiles along the flight track shows a good agreement between both fields. A correlation between ozone and PV on the potential temperature levels, where the filaments were observed, deliver coeffi-

cients that reflect a good agreement in the range of the uncertainties of the lidar measurements and the model input data.

The correlation showed also that the filaments can sometimes be displaced by the PV advection model. A shift of about 500 or 300 s has improved the correlation in the case of the polar filaments on February 18 and March 18, respectively. This time shift corresponds to a spatial difference of about 100 and 60 km, or 0.73° and 0.5°, in both the zonal and the meridional direction. In case of the subtropical intrusion on March 29, a shift of about 100 km northeastward, or 0.73°, was found in the upper levels of the ozone minimum. At the lower levels the position of the intrusion was placed right by the model. On April 6 and 7 the observed displacement is much larger with about 300 km in direction southeast. This corresponds to 3.3° in the zonal and 1.6° in the meridional direction.

Compared to other studies, the displacements found in the data from the METRO airborne campaign lie in the same order of magnitude, except for the last subtropical case on April 6 and 7. For example, *Newman and Schoeberl* [1995] found a correlation of 0.45 between airborne ozone lidar data from the Stratospheric-Tropospheric Exchange project compared to reverse domain filling modeled PV distribution and a displacement of filament structures less than 1° further south than the ozone filament. *Fleitze et al.* [2000] compared the ozone data obtained by the Ozone Lidar Experiment lidar on board the German Falcon during the SESAME campaign in winter 1994/1995 with contour advection

PV advection model MIMOSA on 29.03.1999 at level 380K

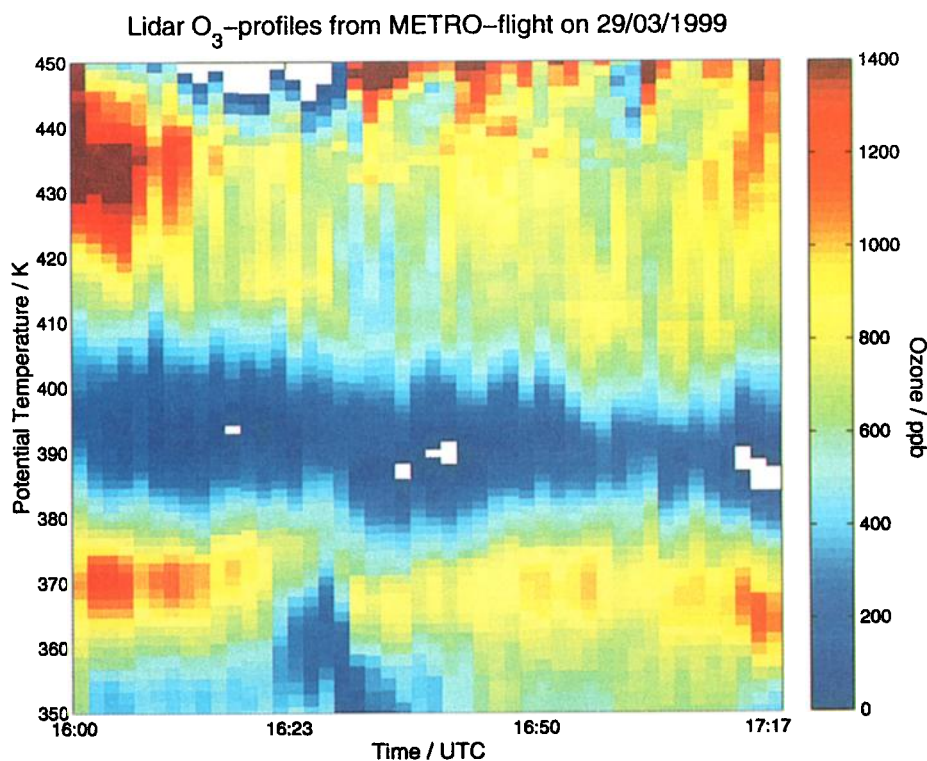
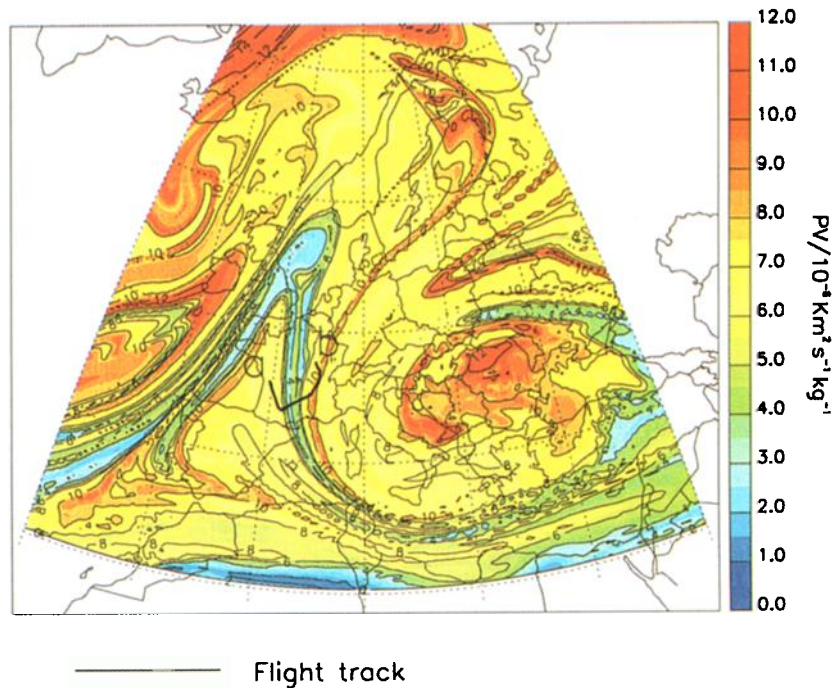


Plate 3. (top) Modeled PV distribution at 380 K on March 29, 1999 at 1600 UTC. Measurements during this round flight startet at point a and ended at point b. (bottom) Measured ozone profiles during the flight on March 29, 1999.

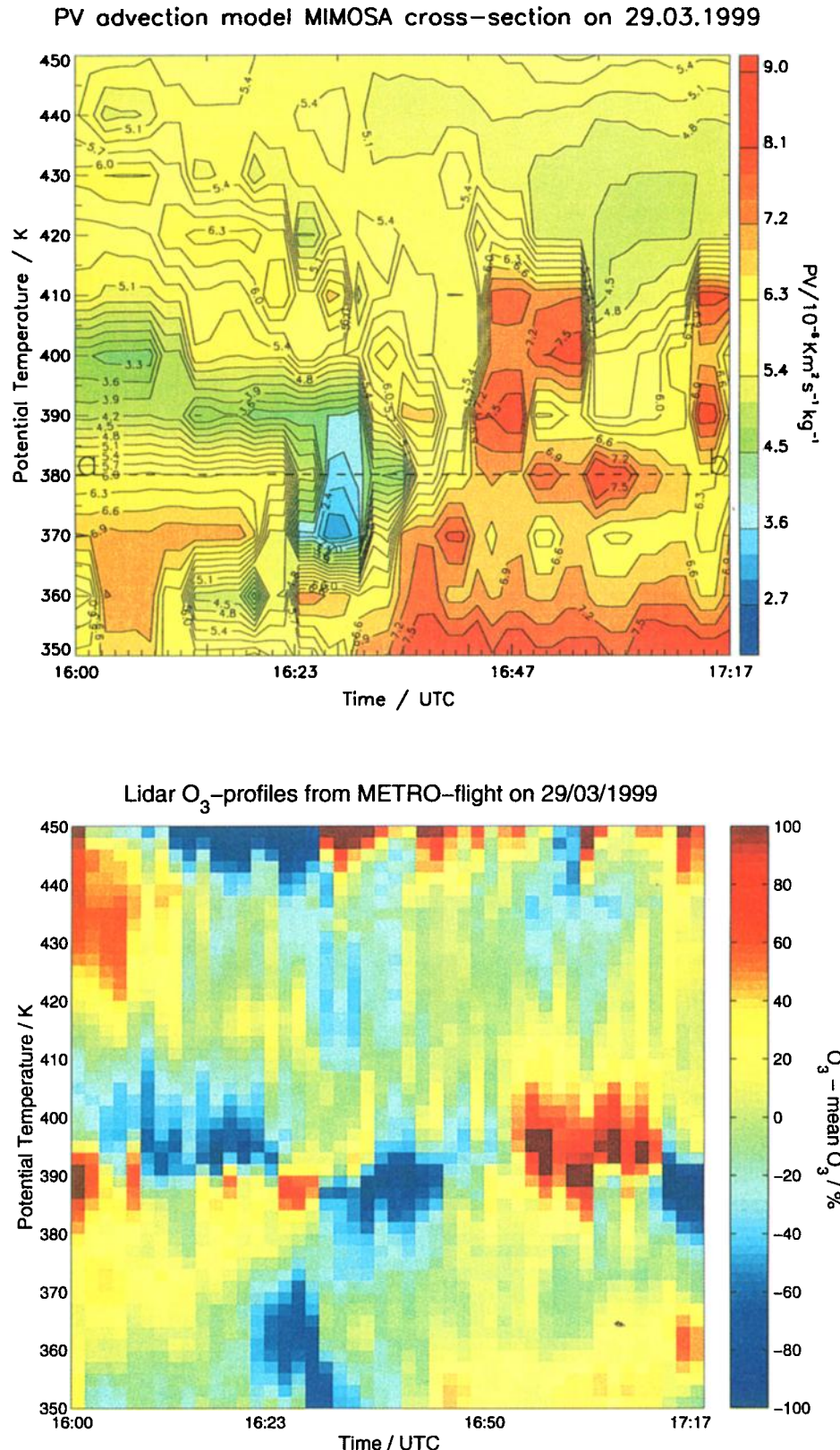


Plate 4. (top) Modified PV cross section during flight on March 29, 1999. The dashed line indicates the level 380 K shown on the horizontal map in Plate 3. (bottom) Ozone anomalies calculated with respect to the mean ozone profile for this flight.

PV cross sections and found a meridional displacement of less than 0.5° in 70% of the cases, and 10% showed a displacement of more than 1° .

A major part of the displacements of the filaments found in the METRO study can be explained by the uncertainties of the input data to the model MIMOSA. A mean error in ECMWF (31 and 50 level version) wind velocity of 2.5 ms^{-1} in the region between 30 and 70 hPa (around 20 km altitude) was found comparing the ECMWF analysis wind vectors to the velocities measured during long-duration balloon flights [Knudsen et al., 1999]. This error leads to a displacement of 7° after 10 days in trajectory calculations. Since the polar filaments observed at 435 K correspond to an altitude around 17 to 18 km, we can assume an error in ECMWF winds of the same magnitude. For the subtropical intrusions at levels around 380 K the error may differ. The displacements observed in MIMOSA for polar filaments at levels around 435 K are much smaller than the ones found for trajectory calculations. Even in the last subtropical case on April 6 and 7 the displacement is only about half the displacement found for the trajectory calculations. This is evident since the errors of the position of the filaments depend less on the wind velocity in the direction of the trajectories but more on the error perpendicular to the direction of the trajectories.

The sensitivity to errors in the wind data of the PV advection model MIMOSA has been estimated for a filament observed in December 1997, (Hauchecorne et al., submitted manuscript, 2001). Two types of errors were assumed: (1) a constant error of 1 ms^{-1} in direction of the wind, and (2) a constant error of 0.2 ms^{-1} perpendicular to the direction of the wind. After 10 days of advection the mean error of the position of a filament, perpendicular and parallel to the filament, has been estimated: For the first case (1 ms^{-1}) the error for the position of the filament was 95 km perpendicular and 295 km parallel to the filament. For the second case (0.2 ms^{-1}) the error was 80 km perpendicular to the filament and 160 km parallel to the filament. These errors compare quite well to the displacements of 60 km and 100 km perpendicular to the filaments found for three of the METRO flights. Regarding the large displacements found for the second subtropical intrusion, a review of the ECMWF wind velocities during the 10 days of advection used in the model showed that the circulation at 380 K in the end of the winter is much more disturbed and errors in the input wind data may be higher.

Finally, we can state that the modeled and observed structures in the PV and ozone fields are of comparable size. Air masses of polar, midlatitude, and subtropical origin were well distinguished by the modeled PV gradients. The position of the filaments could be simulated with small displacements in most cases of 0.5° to 0.7° . The discrepancies between both fields found

in this study can be accounted for by the estimated error in the ECMWF wind fields. The model was used to forecast the filaments and to plan the flights during the METRO campaign, and the predicted polar filaments and subtropical intrusions were always detected by the ozone lidar measurements. Thus the PV advection model MIMOSA is suitable for studies of the meridional transport of polar and subtropical air masses into midlatitudes. A study of the influence of the filamentation processes on the ozone amount will be undertaken including the lidar and ozone sonde measurements of the ground-based station at the Observatoire de Haute Provence (S. Godin et al., Influence of the Arctic polar vortex erosion on the lower stratospheric ozone amounts at OHP (44°N , 6°E), submitted to *J. Geophys. Res.*, 2001). Furthermore, MIMOSA has been used to evaluate the transport of air across the polar vortex edge during the four last winters (Hauchecorne et al., submitted manuscript, 2001).

For further studies, the model was coupled with the chemical part of the French chemical transport model REPROBUS [Lefèvre et al., 1994] to account for the ozone destruction observed in other winters. Observations show very high local ozone loss of over 60% during winter 1999/2000 inside the Arctic polar vortex. Fortunately, the METRO campaign could be extended into winter 2000 in the framework of the European project THESEO 2000, and additional airborne lidar measurements of polar filaments became feasible. Although the stable polar vortex kept the polar air inside its boundaries most of the time, several flights through polar filaments could be performed. These data are still under investigation and will be analyzed using the coupled MIMOSA-REPROBUS model [Marchand et al., 2000] together with the measurements from the ground-based network.

Acknowledgments. We are grateful to G. Ancellet to provide the ALTO lidar and would like to thank the staff at Institute Géographique National (IGN) for the logistics and the performances of the flights. We will also thank our colleagues at Institut National de Science de l'Univers (INSU) who have processed the accompanying flight data. Many thanks to Bernard Legras and his group who provided the PV calculation scheme. Finally, we want to thank Jean Louis Conrad, Anne Garnier, Christian Laqui, Claude Leroy, Jean-Pierre Marcovici, and Jacques Porteneuve for their help concerning the lidar system and data acquisition. Thanks to the suggestions of two anonymous reviewers. Due to their comments the paper has been substantially improved. This work was funded by the European commission through the project THESEO - METRO under contract ENV4-CT97-0529.

References

- Ancellet, G., and F. Ravetta, Compact airborne lidar for tropospheric ozone: Description and field measurements, *Appl. Opt.*, 37, 5509–5521, 1998.
- Butchart, N., and E. E. Remsberg, The area of the stratospheric polar vortex as a diagnostic for tracer transport

- on an isentropic surface, *J. Atmos. Sci.*, **43**, 1319–1339, 1986.
- de Schoulepenkoff, L., V. Mitev, V. Simeonov, B. Calpini, and H. van den Berg, Experimental investigation of high-power single-pass Raman shifters in the ultraviolet with Nd:YAG and KrF lasers, *Appl. Opt.*, **36**, 5026–5043, 1997.
- Flentje, H., W. Renger, M. Wirth, and W. A. Lahoz, Validation of contour advection simulations with airborne Lidar measurements of filaments during the second European Stratospheric Arctic and Midlatitude Experiment (SESAME), *J. Geophys. Res.*, **105**, 15,417–15,437, 2000.
- Holton, J. R., P. H. Haynes, M. E. McIntyre, A. R. Douglas, R. B. Rood, and L. Pfister, Stratosphere-troposphere exchange, *Rev. Geophys.*, **33**, 403–439, 1995.
- Hood, L., S. Rossi, and M. Beulen, Trends in lower stratospheric zonal winds, Rossby wave breaking behavior, and column ozone at northern midlatitudes, *J. Geophys. Res.*, **104**, 24,321–24,339, 1999.
- Knudsen, B. M., J. P. Pommereau, A. Garnier, M. Numez-Pinharanda, L. Denis, F. Nouel, V. Duborg, and G. Letrenne, Comparison of calculated trajectories with long duration balloon data, paper presented at 5th European Workshop on Stratospheric Ozone, European Commission, Saint-Jean-de-Luz, France, Sept. 27 – Oct. 1, 1999.
- Lait, L. R., An alternative form for potential vorticity, *J. Atmos. Sci.*, **51**, 1754–1759, 1996.
- Lefevre, F., G. B. Brassuer, I. Folkins, A. K. Smith, and P. Simon, Chemistry of the 1991–1992 stratospheric winter: Three-dimensional model simulations, *J. Geophys. Res.*, **99**, 8183–8195, 1994.
- Marchand, M., S. Godin, B. Heese, and A. Hauchecorne, A study of polar filaments using the coupled model MIMOSA-REPROBUS, paper presented at Quadrennial Ozone Symposium, EORC/NASDA, Sapporo, Japan, July 3 – 8, 2000.
- Naujokat, B., The winters 1997/98 and 1998/99 in perspective, paper presented at 5th European Workshop on Stratospheric Ozone, European Commission, Saint-Jean-de-Luz, France, Sept. 27 – Oct. 1, 1999.
- Newman, P. A., and M. R. Schoeberl, A reinterpretation of the data from the NASA stratosphere-troposphere exchange project, *Geophys. Res. Lett.*, **22**, 2501–2504, 1995.
- Norton, W. A., and M. P. Chipperfield, Quantification of the transport of chemically activated air from the northern hemispheric polar vortex, *J. Geophys. Res.*, **100**, 25,817–25,840, 1995.
- Orsolini, Y., D. Cariolle, and M. Deque, Ridge formation in the lower stratosphere and its influence on ozone transport: A general circulation model study during late January 1992, *J. Geophys. Res.*, **100**, 11,113–11,135, 1995.
- Papayannis, A. D., G. N. Tsikrikas, and A. A. Serafetinides, Generation of UV and VIS laser light by stimulated Raman scattering in H₂, D₂/He using a pulsed Nd:YAG laser at 355 nm, *Appl. Phys. B*, **67**, 1–7, 1998.
- Reid, S. J., and G. Vaughan, Lamination in ozone profiles in the lower stratosphere, *Q. J. R. Meteorol. Soc.*, **117**, 825–844, 1991.
- Reid, S. J., G. Vaughan, and E. Kyro, Occurrence of ozone laminae near the boundary of the stratospheric polar vortex, *J. Geophys. Res.*, **98**, 8883–8890, 1993.
- Vaughan, G., and C. Timmis, Transport of near-tropopause air into the lower midlatitude stratosphere, *Q. J. R. Meteorol. Soc.*, **124**, 1559–1578, 1998.
- World Meteorological Organization, Scientific Assessment of Ozone Depletion: 1998, in *Global Ozone Research and Monitoring Project, Rep. 14*, Geneva, 1998.
-
- B. Heese, Meteorological Institute, University of Munich, Theresienstr. 37, D-80333 Munich, Germany.
(b.heese@gtco.de)
- S. Godin, Service d'Aeronomie du CNRS, Universite Pierre et Marie Curie, 4, Place Jussieu, Boite 102, F-75252 Paris Cedex 05, France.
(sophie.godin@aero.jussieu.fr)
- A. Hauchecorne, Service d'Aeronomie du CNRS, BP3, F-91371 Verrieres-le-Buisson Cedex, France.
(alain.hauchecorne@aerov.jussieu.fr)

(Received April 14, 2000; revised October 2, 2000;
accepted November 21, 2000.)